

Compositional Sequence Distribution, Cotacticity, and Second-Order Markov Statistics in Vinyl Chloride-Vinyl Acetate Copolymers

Geert van der Velden

Central Laboratory, DSM, Geleen, The Netherlands. Received September 21, 1982

ABSTRACT: ^1H NMR spectroscopy and ^{13}C NMR spectroscopy were used in a detailed study of vinyl chloride-vinyl acetate copolymers. The six methine peaks in the 300-MHz proton spectrum were interpreted in terms of triad compositional sequences. It was observed that with increasing vinyl acetate content, the compositional sequence distribution could be adequately described by a second-order Markov model. From ^1H NMR data, no information could be obtained about the configurational sequence distribution (cotacticity). From the vinyl acetate and vinyl chloride centered methine resonances in the ^{13}C NMR spectra of these copolymers, information could be obtained about cotacticity and compositional sequence distribution.

1. Introduction

Copolymers of vinyl chloride (VC) and vinyl acetate (VA) are more elastic than the homopolymer poly(vinyl chloride) (PVC). Information on the sequence distribution of the VA-VC copolymers has been obtained recently via ^{13}C NMR measurements.^{1,2} Through studies of the three compositional methylene dyads^{1,2} and of the mixed configurational-compositional VA-centered methine triad,¹ quantitative determination of sequence distributions in these polymers has become possible.

A study of the VC-centered methine carbons has been attempted, but no distinction has been made between compositional and configurational effects.² Admittedly, a Bernoullian model can be shown to be consistent^{1,2} and Markov models of any order can be fitted by using methylene dyad data. On the contrary, from compositional methine triad data a first-order Markov model can be tested and higher models can be fitted, but triad information about the VC-centered methine carbon or proton is lacking,^{1,2} so no real discrimination between Bernoullian and Markov statistics can be made.

Recently, van der Velden and Beulen³ showed in a 300-MHz ^1H NMR study that compositional sequence distributions could be obtained from a study of the clearly separated signals of vinyl acetate and vinyl alcohol (VA-VOH) centered methine protons. It is the purpose of this paper to show that the same method can also be successfully employed to study these VA-VC copolymers. Moreover, detailed information about cotacticity (not obtained from 300-MHz ^1H NMR measurements) could be obtained from 50-MHz ^{13}C NMR spectra.

2. Experimental Section

VA-VC copolymers were obtained from Wacker (Vinnol H10/60 and Vinnol 4055 T), respectively coded as A and B, and used as such.

The 100-MHz ^1H NMR spectra were measured with a Varian XL-100/12-A spectrometer, operating in the CW mode. The 300.25-MHz ^1H NMR spectra were measured with a Varian SC-300 spectrometer⁴ at 85 °C, using perdeuterated dimethyl sulfoxide ($\text{Me}_2\text{SO}-d_6$, Merck) as solvent and as internal locking agent. Five-millimeter tubes were used. The sweep width of the spectrometer operated in the FT mode amounted to 3500 Hz and the acquisition time to 2 s, and a pulse delay of 5 s and a pulse width of 3 μs (33° flip angle) were chosen. These parameters were determined by trial and error by equalizing the results obtained for the copolymer composition with the results from 100-MHz ^1H CW NMR spectra recorded for the same sample. The sample concentration was 3% (w/v) and 20 transients were stored. The 50.309-MHz ^{13}C NMR spectra were obtained with a Varian XL-200 spectrometer equipped with a V-77-200 Sperry Univac computer. The sample concentration was 9% (w/v) in either $\text{Me}_2\text{SO}-d_6$ or C_6D_6 . Using 10-mm tubes, ^{13}C NMR spectra were

recorded at 50 °C in C_6D_6 as solvent and in $\text{Me}_2\text{SO}-d_6$ at 85 °C. The pulse width (13 μs) corresponds to a flip angle of 90°, and a pulse delay of 5 s was found to be necessary. Spectra were generally obtained after the accumulation of 10 000 FIDS, where the digital resolution amounted to 0.687 Hz/point, corresponding to a spectral width of 11 000 Hz and a data length of 16K. Peak areas were determined via planimeter or integration methods, after curve resolution with Lorentzian lines. Monomer sequence distributions and configurational sequence placements were determined by comparing the relative intensities of the protons or carbons involved. In performing quantitative NMR measurements, it is necessary to take differences in nuclear Overhauser effects (NOE) and spin-lattice relaxation times (T_1) into account. No proton T_1 's and no carbon T_1 's and NOEs have been measured by us, because these NOEs and T_1 's have been measured already by Okada et al.¹ for the different types of carbons (excluding the carbonyl carbon) present in or near the copolymer main chain. The NOEs for all proton-bearing carbons agree, within experimental error, with the theoretically calculated values (at 50 °C in C_6D_6 , 25 MHz). No differential NOEs were observed for the methylene carbons. The T_1 values for the methine, methylene, and methyl carbons are (VA = 0.22) 0.12, 0.06, and 0.80 s, respectively, and increase slightly with increasing VA content.¹ Bearing this in mind, we have run these copolymers with a long delay time (5 s) and calculated the copolymer composition via measurements of methyl and methine carbon peak areas and via measurements of the VC- and VA-centered methine carbon peaks separately. The results are identical with those obtained via ^1H NMR.

The 5.0-s delay time probably does not allow full recovery of the carbonyl carbons, but no configurational- or compositional-induced splitting, similar to those found for VA-VOH copolymers,³ occurred.

Implicitly it has been assumed that no different spin-lattice relaxation times are present for different stereoisomeric (mm, mr, and rr) or compositional ((VA, VA, VA), (VA, VA, VC), and (VC, VA, VC)) sequences in the methine-centered resonances in the ^1H and ^{13}C NMR spectra.

No differential ^1H NOEs have been considered to occur. Within these limits relative peak areas are proportional to the numbers of protons and carbon atoms involved.

3. Results and Discussion

A. ^1H NMR Spectra of VA-VC Copolymers. Figure 1 depicts the 300-MHz ^1H NMR spectra of two VA-VC copolymers dissolved in $\text{Me}_2\text{SO}-d_6$ at 85 °C.

Using the results from double-resonance experiments and assignments for PVC,¹ poly(vinyl acetate) (PVA),⁵ and vinyl alcohol-vinyl acetate copolymers,³ it is a relatively straightforward operation to assign all resonances. The complete assignment is given in Table I and will be discussed in some detail now. In the following sections, the two kinds of monads and their mole fractions will be denoted by VA and VC, while the three kinds of dyad sequences and their mole fractions will be given by (VC, VC),

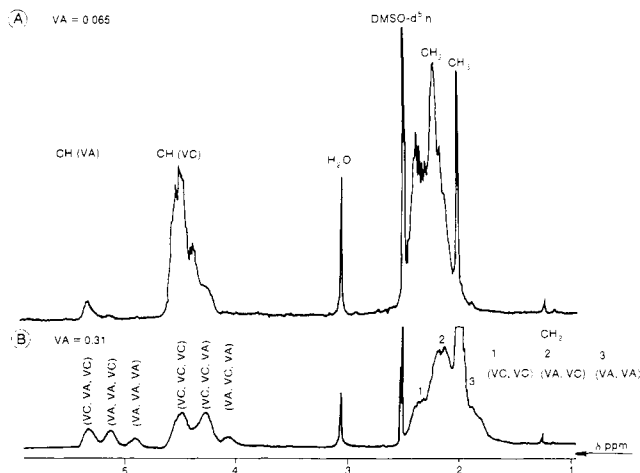


Figure 1. 300-MHz ^1H NMR spectra of vinyl chloride-vinyl acetate copolymers in $\text{Me}_2\text{SO}-d_6$ at 85°C .

Table I
Spectral Assignments for Vinyl Chloride-Vinyl Acetate Copolymers As Measured via 300-MHz ^1H NMR

chem shift, ^a ppm	protons	dyads or triads
2.01	methyl	(VA, VA, VA), (VA, VA, VC), (VC, VA, VC)
1.96	methylene	(VA, VA)
2.14	methylene	(VA, VC)
2.34	methylene	(VC, VC)
4.03	methine	(VA, VC, VA)
4.23	methine	(VC, VC, VA)
4.45	methine	(VC, VC, VC)
4.86	methine	(VA, VA, VA)
5.07	methine	(VA, VA, VC)
5.27	methine	(VC, VA, VC)

^a Chemical shift is given with respect to internal $\text{Me}_2\text{SO}-d_6$ (2.50 ppm).

(VA, VC), and (VA, VA). A similar notation is used for the six different kinds of triads, e.g., (VC, VC, VC), (VA, VC, VC), (VA, VA, VA), etc.

The methylene proton resonances, centered at 1.96, 2.14, and 2.34 ppm, are rather broad due to a combination of spin-spin coupling and configurational splittings but can be assigned to three compositional dyads (see Figure 1). Quantitative information about the methylene dyads is also hard to extract as a consequence of the overlap with the methyl proton resonance and is more easily obtained from an analysis of the ^{13}C NMR methylene dyad data.

Not counting resonances that are due to $\text{Me}_2\text{SO}-d_6$ and H_2O , the number of the remaining resonances visible is six, in two separate groups of three lines. These resonances are all due to methine protons.¹ As already apparent from the 100-MHz spectra recorded earlier,¹ the VA and VC methine centered resonances are separated by approximately 1 ppm. Moreover, the three resonances in a particular group can be easily assigned because the configurational splitting, observed in the 200- and 300-MHz spectra of PVC,¹ PVA,⁵ and VA-VOH copolymers,^{3,6} only contributes to the line width. Therefore, exactly similar to the assignments of the VA-VOH copolymers, all six methine resonances for these VA-VC copolymers have been assigned to six compositional triads. The relative peak areas for the methine-centered resonances are given in Table II. From the methine data the mole fraction (VA) can be derived by using eq 2 of ref 1.

The results obtained via 300-MHz ^1H NMR are in good agreement with those from 100-MHz CW NMR and those

Table II
Composition and Mole Fractions of Dyads and Triads As Measured and Calculated via ^1H NMR and ^{13}C NMR of Vinyl Chloride-Vinyl Acetate Copolymer B (VA = 0.31)

	^1H NMR ^a	^{13}C NMR ^b
(VC, VC, VC)	0.329	
(VC, VC, VA)	0.302	
(VA, VC, VA)	0.055	
(VC, VA, VC)	0.139	
(VA, VA, VC)	0.116	
(VA, VA, VA)	0.055	
(VC, VC)		0.47
(VA, VC)		0.40
(VA, VA)		0.13
n_0^{VA}	1.57	1.65
n_{2+}^{VA}	2.95	
n_0^{VC}	3.34	3.35
n_{2+}^{VC}	4.18	
(VA)	0.31	0.32

^a In $\text{Me}_2\text{SO}-d_6$. ^b In C_6D_6 .

obtained via a chlorine analysis using the Schöniger flask method.⁷ Moreover, from the methine-centered resonances additional information can be acquired about the number-average acetate sequence length (n_0^{VA}) and about the number-average sequence length of acetyl side chains higher than two (n_{2+}^{VA}). Similar formulas^{3,8} also hold for the chloro side chains, n_0^{VC} and n_{2+}^{VC} , respectively, via mutual cyclic permutations. The results for sample B (Vinnol 4055T, VA = 0.31) are given in Table II.

In order to explore the comonomer arrangements for VA-VC copolymers, we examine Bernoullian and Markovian analyses. A second-order Markov process requires the specification of eight conditional probabilities, for we must consider the influence of the composition of the last three units of the growing chain end. For convenience, we designate these as⁹

$$\begin{aligned}
 P(\text{VCVC}/\text{VC}) &= \alpha & P(\text{VCVC}/\text{VA}) &= \bar{\alpha} \\
 P(\text{VCVA}/\text{VC}) &= \beta & P(\text{VCVA}/\text{VA}) &= \bar{\beta} \\
 P(\text{VAVC}/\text{VC}) &= \gamma & P(\text{VAVC}/\text{VA}) &= \bar{\gamma} \\
 P(\text{VAVA}/\text{VC}) &= \delta & P(\text{VAVA}/\text{VA}) &= \bar{\delta}
 \end{aligned} \quad (1)$$

where $P(\text{VCVC}/\text{VC})$ is the probability of a VC monomer joining a chain end terminating in VCVC, and so on.

We calculate for the observable compositional triad sequences

$$\begin{aligned}
 \text{VCVCVC} &= \alpha\gamma\delta s^{-1} \\
 \text{VCVCVA} &= 2\bar{\alpha}\gamma\delta s^{-1} \\
 \text{VAVCVA} &= \bar{\alpha}\bar{\gamma}\delta s^{-1} \\
 \text{VCVAVC} &= \bar{\alpha}\beta\delta s^{-1} \\
 \text{VCVAVA} &= 2\bar{\alpha}\bar{\beta}\delta s^{-1} \\
 \text{VAVAVA} &= \bar{\alpha}\bar{\beta}\bar{\delta} s^{-1} \\
 s &= \bar{\alpha}\bar{\beta} + 2\bar{\alpha}\delta + \gamma\delta
 \end{aligned} \quad (2)$$

This second-order Markov model reduces to a first-order Markov model when $\alpha = \gamma$ and $\beta = \delta$ and to a Bernoullian model if $\alpha = \beta = \gamma = \delta$.⁹ These relationships (eq 2) can be used for testing experimentally determined peak areas for conformity to these propagation statistics. The experimentally observed (^1H NMR) and theoretically calculated values are given in Table III for polymers A and

Table III
Calculated and Observed Triad Comonomer Distributions for Vinyl Chloride-Vinyl Acetate Copolymers^a

triad	obsd distribution	Bernoullian ^d	first-order Markov ^e	second-order Markov ^f
VCVCVC ^b	0.814	0.817		
VCVCVA	0.121	0.114		
VAVCVA	0.000	0.004		
VCVAVC	0.055	0.057		
VAVAVC	0.010	0.008		
VAVAVA	0.000	0.000		
VCVCVC ^c	0.329	0.328	0.316	0.332
VCVCVA	0.302	0.295	0.284	0.299
VAVCVA	0.055	0.066	0.064	0.053
VCVAVC	0.139	0.148	0.125	0.143
VAVAVC	0.116	0.133	0.160	0.117
VAVAVA	0.055	0.030	0.051	0.056

^a For discussion, see text. ^b ¹H NMR data. ^c VA = 0.065 (A). ^d VA = 0.31 (B). ^e $\alpha = 0.935$ (VA = 0.065), $\alpha = 0.69$ (VA = 0.31). ^f $\alpha = \gamma = 0.69$, $\beta = \delta = 0.61$. ^f $\alpha = 0.69$, $\beta = 0.71$, $\gamma = 0.74$, and $\delta = 0.51$.

B, using Bernoullian analysis (A: $\alpha = 0.935$; B: $\alpha = 0.69$) and Markovian analyses (B: first order, $\alpha = \gamma = 0.69$, $\beta = \delta = 0.61$; second order, $\alpha = 0.69$, $\beta = 0.71$, $\gamma = 0.74$, and $\delta = 0.51$). The estimated accuracy of the experimentally determined peak areas for polymers A and B has been assumed to be 0.01 and 0.005, respectively.

It is evident that for polymer B (VA = 0.31) the Bernoullian model can be abandoned and that a significant amelioration of the results is achieved by going from first-order Markov to second-order Markov analyses. Thus the propagation statistics of polymer B is adequately described by a second-order Markov process. A Bernoullian model is sufficient to describe the propagation statistics of polymer A (VA = 0.065). However, it has to be noted that significant deviations from a Bernoullian model only occur for polymer B in the compositional sequences (VA, VA, VC) and (VA, VA, VA); these sequences are hardly or not at all present in polymer A. Therefore discrimination between the two models cannot be made.

According to Figure 10 of ref 1 significant deviations also exist between experimentally observed (¹³C NMR) and values calculated via a Bernoullian model, for copolymers containing mole percentages VA higher than 20%. The differences occur only for the same compositional sequences (VA, VA, VC) and (VA, VA, VA), but Okada et al.¹ did not pay any attention to these (slight) deviations. These deviations can now be explained by using the Markovian analysis.

B. ¹³C NMR of VA-VC Copolymers. Figure 2 shows the 50-MHz ¹³C NMR spectra of polymers A and B recorded in Me₂SO-*d*₆ and of polymer B in C₆D₆ with and without the presence of the shift reagent Pr(fod)₃. Only the methine, methylene, and methyl regions are shown, since no configurational- or compositional-induced splitting of the carbonyl resonance is observed either for Me₂SO-*d*₆ or for C₆D₆. The Me₂SO-*d*₆ signal severely distorts the methylene dyads. The assignment has already been accomplished by Okada et al.¹ and partly by Schlothauer and Alig² (excluding the VC methine centered resonances) and is reproduced in Figure 2.

The mole fraction (VA), n_0^{VA} , and n_0^{VC} can be calculated from methylene dyad data^{3,6,8} and are given in Table II. However, compositional sequence determination is not a priori possible for the VC and VA methine centered resonances. Therefore, n_0^{VC} and n_0^{VA} have not been calculated from the ¹³C NMR spectra because the mixed configurational-compositional VC methine triad (cf. Figure 2) has not been unraveled¹ or has been tentatively attributed to exclusively configurational sequences.² Under the present measuring conditions, the ten possible VC-

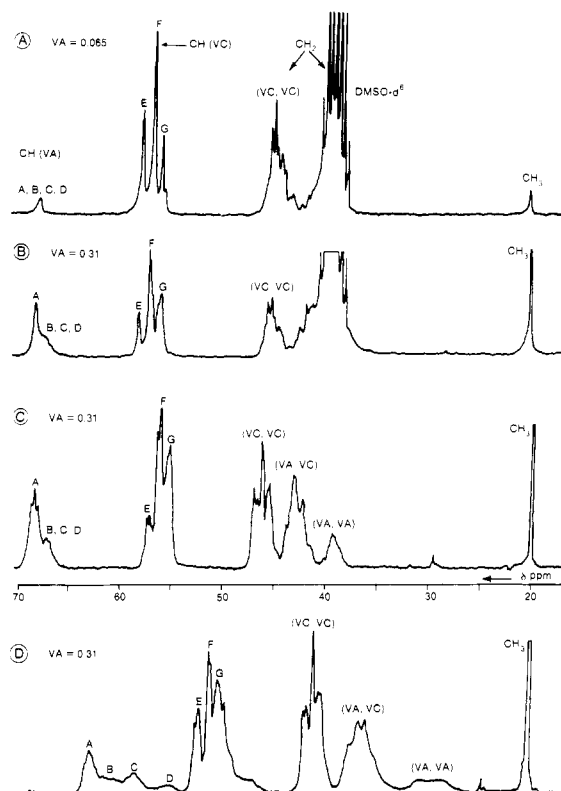


Figure 2. 50-MHz ¹³C NMR spectra of vinyl chloride-vinyl acetate copolymers in Me₂SO-*d*₆ at 60 °C (A, B) and in C₆D₆ at 50 °C (C, D), (C) without and (D) with the presence of 0.50 M Pr(fod)₃. The assignments A-G are discussed in the text.

centered triads give rise to only three methine resonances (in Me₂SO-*d*₆ and THF²) or five (in C₆D₆).¹ Knowing the experimental peak areas for the VC-centered resonances (¹H NMR, Table III) allows us to arrive at the following set of equations (m^{11} = meso(VC, VC) and m = meso(VA, VC)):

$$E = r^{11}r^{11}(\text{VC, VC, VC})$$

$$F = 2m^{11}r^{11}(\text{VC, VC, VC}) + (rr^{11} + mr^{11})(\text{VA, VC, VC})$$

$$G = m^{11}m^{11}(\text{VC, VC, VC}) + (m^{11}r + m^{11}m)(\text{VA, VC, VC}) + (mm + 2mr + rr)(\text{VA, VC, VA}) \quad (3)$$

In eq 3, *E*, *F*, and *G* represent the measured areas of the VC-centered resonances in the ¹³C NMR spectrum at respectively low, central, and high field. This set of equa-

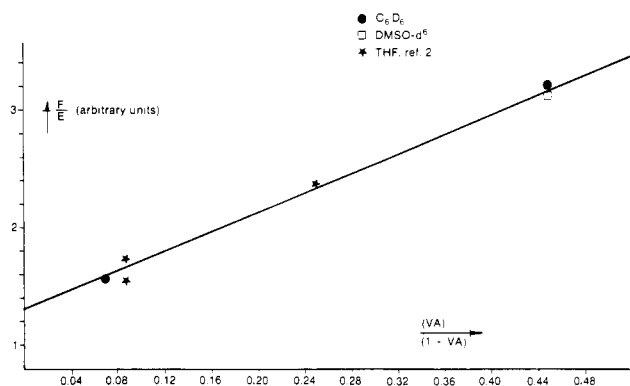


Figure 3. Ratio of the central field and low field relative peak areas of the vinyl chloride centered methine ^{13}C resonances vs. the ratio $(\text{VA})/(1 - \text{VA})$.

Table IV
Relative Peak Areas of the VC Methine Centered ^{13}C Resonances for Copolymers A and B

	polymer A		polymer B		
	exptl ^a	theor ^c	exptl ^a	exptl ^b	theor ^a
low field (E)	0.31	0.31	0.15	0.15	0.17
central field (F)	0.49	0.50	0.48	0.46	0.49
high field (G)	0.20	0.10	0.37	0.39	0.34

^a Measured in $\text{Me}_2\text{SO}-d_6$. ^b Measured in C_6D_6 . ^c Calculated using eq 3, substituting $m^{11} = 0.40$, and via the ^1H NMR experimentally determined compositional triads.

tions is exactly identical with the earlier proposed assignments of the carbonyl triple region in the ^{13}C NMR spectra of VA-VOH copolymers.^{3,6} In the VA-VC and VA-VOH systems, the downfield shift is caused by VC or VOH groups being present in racemic positions.

Equation 3 can be put in a handier form, assuming Bernoullian statistics to hold:

$$\frac{F}{E} = \frac{2m^{11}}{r^{11}} + \frac{2}{r^{11}} \left(\frac{\text{VA}}{1 - \text{VA}} \right) \quad (4a)$$

Figure 3 presents a plots of F/E vs. $(\text{VA})/(1 - \text{VA})$ and verifies to a certain extent the assignments. Note that also two values, given by Schlothauer and Alig,² have been taken into account. From the slope or the intercept the value m^{11} can be calculated: $m^{11} = 0.40$. Substituting the various parameters $m^{11}m^{11}$, $2m^{11}r^{11}$, and $r^{11}r^{11}$, together with the experimentally determined values for the VC methine centered compositional triads (see Table III), in eq 3 leads to calculated intensities in the ^{13}C NMR spectrum that agree quite well with the experimental areas E , F , and G , proving the above assignment (Table IV).

The value of $m^{11} = 0.40$ agrees quite well with the results obtained for free radical polymerized PVC⁸ ($m^{11} = 0.45$). Moreover, this value ($m^{11} = 0.40$) is not very dependent on the type of polymerization process (second-order Markov vs. Bernoulli) because the values for the compositional triads (VC, VC, VC) and (VC, VC, VA) are approximately the same for both types of polymerization statistics (cf. polymer B, Table III).

A calculation for VA-VC copolymers, containing mole percentages $\text{VA} = 0.55$ and $\text{VA} = 0.68$, using $m^{11} = 0.40$ leads to values for E , F , and G being respectively 0.07, 0.39, and 0.54 ($\text{VA} = 0.55$) and 0.04, 0.31, and 0.65 ($\text{VA} = 0.68$). These values are (at least) qualitatively in agreement with the area ratios (visual inspection) to be derived from Figure 2 and Figure 4 of ref 1. Unfortunately, expanded spectra of these copolymers are not available.¹⁰ Assuming ($r^{11}/$

$m^{11}(\text{VA}) \ll 1$, eq 4a can be approximated via a Taylor expansion:

$$\frac{2E}{F} = \frac{r^{11}}{m^{11}} - \frac{r^{11}}{(m^{11})^2}(\text{VA}) + \left(\frac{r^{11}}{m^{11}} \right)^2 (\text{VA})^2 \quad (4b)$$

For commercially important PVC-rich copolymers ($0 \leq \text{VA} \leq 0.1$) even a linear relationship could be anticipated. In fact, an empirically found graph of $2E/F$ vs. (VA) has been published,² but these authors equalized $2E/F$ erroneously with r^{11}/m^{11} , therefore reaching the conclusion that the syndiotacticity of the PVC sequences appears to decrease with increasing VA content. A similar plot for our samples leads to a value of $m^{11} = 0.42$, in good agreement with $m^{11} = 0.40$.

Okada et al.¹ have shown that the VA centered methine resonances in the ^{13}C NMR spectrum contain compositional as well as configurational information. These authors used $\text{Pr}(\text{fod})_3$ as a shift reagent to improve the resolution of these signals. A specific example, using the same procedure, is given in Figure 2 for copolymer B. If the alphabetic notation of the four resonances is given by A-D (increasing from low to high field), the following set of equations is arrived at for the VA methine region (cotactic definition).¹

$$A = (mm + 2mr + rr)(\text{VC}, \text{VA}, \text{VC})$$

$$B = (mm^1)(\text{VA}, \text{VA}, \text{VC})$$

$$C = (mr^1 + rm^1 + rr^1)(\text{VA}, \text{VA}, \text{VC}) + m^1m^1(\text{VA}, \text{VA}, \text{VA})$$

$$D = (1 - m^1m^1)(\text{VA}, \text{VA}, \text{VA}) \quad (5a)$$

or alternatively

$$\frac{B+C}{B} = \frac{1}{mm^1} + \frac{D}{B} \frac{(m^1)^2}{(1 - (m^1)^2)} \quad (5b)$$

where m and m^1 denote the probabilities of finding meso (VA, VC) and (VA, VA) dyads, respectively.

Equations 5a can be solved numerically for m and m^1 using the experimental values of the VA methine centered resonances (300-MHz ^1H NMR, Table III) for each copolymer and the measured ^{13}C NMR peak areas $A \dots D$. Without explicit knowledge of the VA-centered compositional triads, a graphical analysis can be used (eq 5b), assuming the values m and m^1 to be constant over a whole series of copolymers.¹

The measured relative peak areas of A , B , C , and D can be derived from Figure 2d and are found to be $A = 0.49$, $B = 0.05$, $C = 0.32$, and $D = 0.14$ (sample B). A numerical calculation using the experimentally observed VA comonomer distribution (Table III) and the measured relative areas A , B , C , and D leads to $m^1 = 0.46$ and $m = 0.29$. The value of $m = 0.29$ for the VA-VC copolymer indicates the existence of strong cosyndiotacticity for VA-VC units, whereas the values of $m^1 = 0.46$ and $m^{11} = 0.40$ imply a slight tendency for more racemic placements of VA-VA and VC-VC units. This result ($m^1 = 0.46$) agrees favorably well with the result obtained for PVA,⁸ and the values for m and m^1 (0.29 and 0.40) correspond closely to the values of $m = 0.39$ and $m^1 = 0.34$, obtained by earlier workers.¹

The consistency of the compositional dyad-triad relations, reflected in the values of n_0^{VA} , n_0^{VC} , n_{2+}^{VA} , and n_{2+}^{VC} shows that head-to-head or tail-to-tail fragments are hardly or not at all present in these systems. Moreover, as seen from the ^1H and ^{13}C NMR spectra (Figures 1 and 2), no evidence is evoked for the presence of side-chain branching.

^1H NMR spectra therefore give detailed information about the compositional sequence distributions, and ^{13}C

NMR spectra give information about the configurational sequences (cotacticity).

Acknowledgment. The author expresses his gratitude to Mrs. A. Vliegen, Mrs. G. Kolfshoten, and Mr. J. Beulen for their enthusiastic assistance.

Registry No. VA-VC copolymer, 9003-22-9.

References and Notes

- (1) Okada, T.; Hashimoto, K.; Ikushige, T. *J. Polym. Sci., Polym. Chem. Ed.* **1981**, *19*, 1821 and references therein.
- (2) Schlothauer, K.; Alig, I. *Polym. Bull.* **1981**, *5*, 299.

- (3) van der Velden, G.; Beulen, J. *Macromolecules* **1982**, *15*, 1071.
- (4) The 300-MHz ^1H NMR spectral measurements were carried out on a Varian SC-300 spectrometer of the Hoofddeling Maatschappelijke Technologie of TNO at Delft, The Netherlands.
- (5) Wu, T. K.; Ovenall, D. W. *Macromolecules* **1973**, *6*, 582.
- (6) Toppet, S.; Lemstra, P. J.; van der Velden, G. *Polymer* **1983**, *24*, 507.
- (7) ASTM Method, E 442-74, 1974.
- (8) Randall, J. C. "Polymer Sequence Determination. ^{13}C NMR Method"; Academic Press: London, 1977; pp 105, 109.
- (9) Frisch, H. L.; Mallows, G. L.; Heatley, F.; Bovey, F. A. *Macromolecules* **1968**, *1*, 533.
- (10) Okada, T., personal communication (1982).

On the Statistics and Dynamics of Confined or Entangled Stiff Polymers

Theo Odijk

Department of Physical and Macromolecular Chemistry, Gorlaeus Laboratories, University of Leiden, 2300 RA Leiden, The Netherlands. Received November 22, 1982

ABSTRACT: The statistics of a wormlike chain of persistence length P and contour length L trapped in a cylindrical pore of diameter D can be understood if a length scale $\lambda \simeq D^{2/3}P^{1/3}$ is introduced ($P \gg D$). If $L \lesssim \lambda$, it is a good approximation to view the chain as being completely rigid. Whenever $L \gg \lambda$, it is convenient to regard the stiff coil as a sequence of rigid links, each of length λ . The free energy involved in forcing a stiff chain into a pore is calculated by scaling arguments. When the chain is confined in a network of mesh size A , we again have $\lambda \simeq A^{2/3}P^{1/3}$. If $L \lesssim \lambda$, it is reasonable to approximate the chain as a completely stiff rod in its reptational and reorientational motion. Whenever $\lambda \lesssim L \lesssim P$, a new region emerges in between the rigid rod and flexible chain limits. Then, the rotational diffusion coefficient scales as L^{-2} instead of L^{-6} as in the rigid rod case. The usual L^{-3} dependence (flexible coil limit) is recovered if $L \gtrsim P$.

Introduction

In spite of its apparent complexity, the dynamics of entangled flexible chains is nowadays understood, semi-quantitatively at least, thanks to the seminal ideas of de Gennes¹ and Edwards.² One can imagine one of the chains to be confined within a virtual tube² formed by the topological restrictions due to the surrounding coils. This test chain reptates, i.e., slithers back and forth along the tube because of Brownian motion, a process that implies a continual modification of the original tube at both its ends (see Chapter 8 of ref 3). Of course, one assumes the restrictive environment to remain fixed during the reptation time, the characteristic time scale of motion of the test chain, but this supposition appears to be reasonable.⁴ These concepts have been developed into an extensive theory^{5,6} although several authors⁶⁻⁸ have attempted to amend the basic reptation mechanism because of the (slight) disparity between various theoretical and experimental exponents.^{3,9}

Doi¹⁰⁻¹² applied the same reasoning to the dynamics of entangled, rigid rodlike macromolecules. His result is that the rotational diffusion coefficient, D_r , of the rods depends spectacularly on the rod length, L . Experimentally, this appears to be confirmed.¹³⁻¹⁶ However, a closer look at the experiments proves that serious discrepancies arise, a fact in large part motivating our own work. At this stage, it is worthwhile to discuss this point in some detail. Zero and Pecora¹⁶ have studied dilute and semidilute solutions of poly(γ -benzyl L-glutamate) in 1,2-dichloroethane by dynamic light scattering. The onset of entanglement as defined by a marked increase in the rotational diffusion coefficient, D_r , occurs at a concentration c^*_{exp} fully 2 orders of magnitude greater than the concentration c^* given by Doi and Edwards.¹¹ Moreover, the molecular weight de-

pendence of c^*_{exp} is much less than that of c^* . In Figure 5 of ref 16, one can see that at a certain concentration, c^{**} , D_r apparently becomes independent of L . Zero and Pecora argue that the slopes instead of the absolute values within the region $c^*_{\text{exp}} < c < c^{**}$ should be used in order to test the Doi-Edwards theory, but this leaves the large finite value of D_r at c^{**} unexplained. Their equation (V.1) has no bearing on this problem because it refers to a zero value of D_r at a finite concentration. Assuming for the sake of argument that the slopes can be used, one ends up with a numerical discrepancy of the order of 1000 and a significantly smaller dependence of D_r on L . References 13-15 also clearly bear out the inadequacies of applying the congested rigid rod theory of Doi and Edwards to real systems.

One rationalization¹⁷ has been to replace L by an effective smaller length ϵL with $\epsilon = \mathcal{O}(0.1)$. This implies that the rods will start hindering each other only at much higher concentrations. A further implication would be that 100 rods of length L enclosed in a volume of order L^3 are not entangled, which we feel is preposterous. A realistic value of ϵ is perhaps 0.5 but certainly not much lower.

Hydrodynamic screening has also been neglected.¹⁸ This is expected to modify various features of the $D_r(L, c)$ function, but the discrepancies noted above are much too large to be explained in this way.

A third and very likely explanation is the influence of the slight flexibility of real macromolecules near the rod limit as has been alluded to previously.¹³⁻¹⁸ Stiff polymers in solution always have a finite persistence length P . One would think that a polymer of length $L = 0.1P$, say, should always behave as a rigid rod. This notion turns out to be incorrect. We shall show that the basic rigidity length scale λ (which we shall call the deflection length) is a function